Interior crises in a dripping faucet experiment

R. D. Pinto,* W. M. Gonçalves, J. C. Sartorelli,† and I. L. Caldas
Instituto de Física da Universidade de São Paulo, Caixa Postal 66318, 05315-970, São Paulo, SP, Brazil

M. S. Baptista
Institute for Physical Science and Technology, University of Maryland at College Park, College Park, Maryland 20742
(Received 5 March 1998)

The existence of a spiraling saddle point and its manifolds in attractors of a leaky faucet experiment is topologically shown. Two interior crises concerning a subtle expansion of the attractor that collides with a stable manifold of this saddle point are reported. [S1063-651X(98)00309-2]

PACS number(s): 05.45.+b, 47.52.+j

A wide class of complex behaviors has been found in the drop-to-drop interval time series of leaky faucet experiments, as periodic and nonperiodic attractors, bifurcations, intermittences, interior and boundary crises, and long range anticorrelations [1–11]. The one-dimensional spring-mass model developed by Shaw and co-workers [1,2] is too simple to give us information about some peculiar structures observed experimentally such as saddle points. As we can just measure the time interval (T_n) between successive drops we have a naturally discrete system, described by events series $\{T_n\}$. Therefore, it is not possible to apply the characterization techniques suitable by flow equations. We searched the experimental attractor for critical points by following the clues given by the construction point by point of its first return map.

Details of the experimental apparatus can be found in Refs. [7,10]. We took a sequence of 47 series of increasing dripping rates (around 25 drops/s), named $E0$ up to $E46$, each one 8192 interdrop times long.

Figure 1 displays first return maps (T_{n+1} vs T_n) of four characteristic attractors (chosen among the 47 obtained). On the basis of their similarities we split the set of attractors into three groups: from $E0$ up to $E23$ [Fig. 1(a)], from $E24$ up to $E33$ [Figs. 1(b) and 1(c)], and the last group from $E34$ up to $E46$ [Fig. 1(d)]. Inside each group the attractors' profiles are similar, with a smooth evolution of the mean dripping rate, as shown in Fig. 2. However, there are sudden changes in the dripping rate in the transition between neighboring groups.

Concerning the attractor change from Fig. 1(a) to Fig. 1(b), the attractor increased in size but its shape changed only slightly. The previous structure is still apparent in Fig. 1(b) since the orbits of the expanded attractor spend most of iterates in the original region.

The application of the false nearest-neighbor algorithm [12] results in an embedding dimension equal to 3. Therefore, we analyzed the attractors in tridimensional return maps (T_{n+2} vs T_{n+1} vs T_n). In Fig. 3(a) is shown the map for the

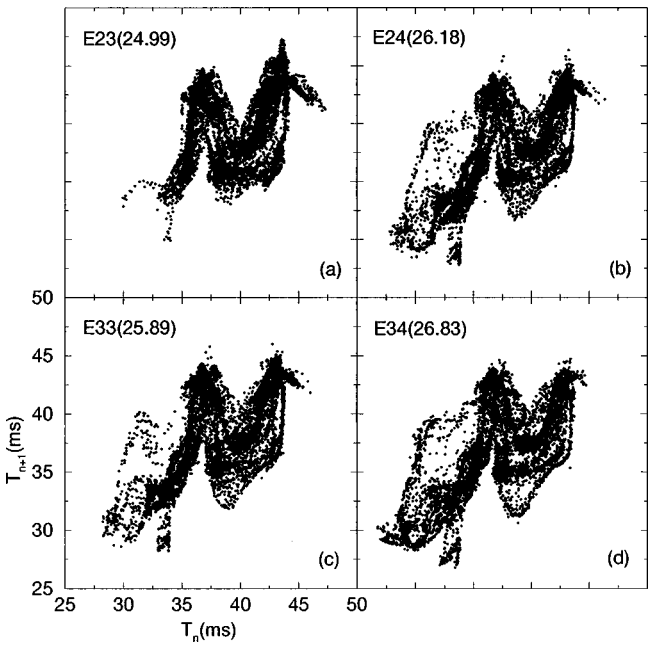

FIG. 1. First return maps T_{n+1} vs T_n representing three identified groups of attractors. (a) belongs to the group before the first interior crisis, (b) and (c) belong to the group between the first and the second interior crises, and (d) belongs to the group after the second crisis. The numbers in parenthesis are the dripping rates.

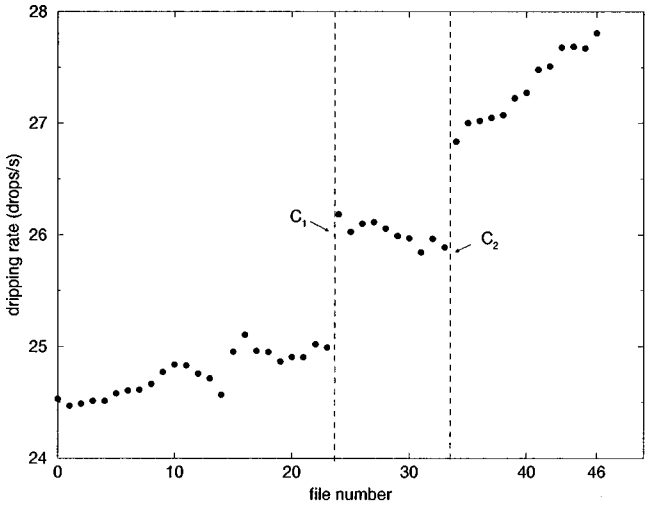

FIG. 2. Dripping rate as a function of file number (faucet opening). The sudden changes in the dripping rate (C_1 and C_2) correspond to the first and second interior crises.

*Electronic address: reynaldo@fge.if.usp.br
†Electronic address: sartorelli@if.usp.br

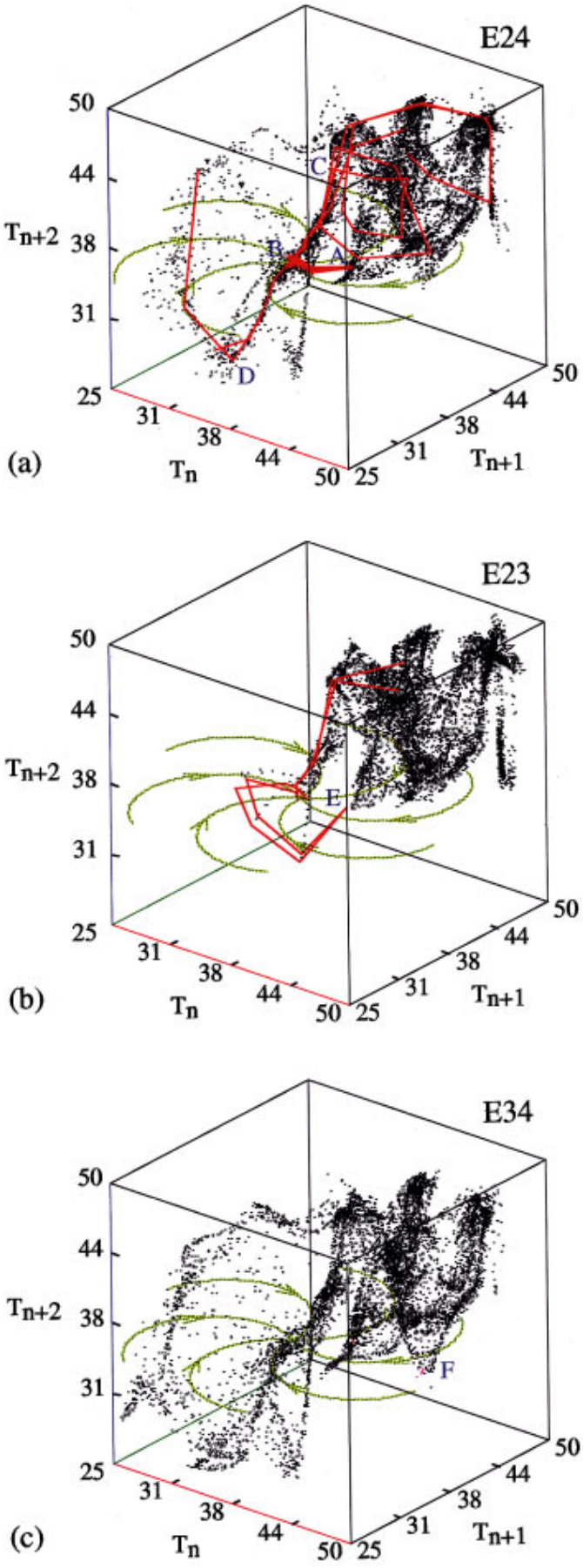

FIG. 3. (Color) Tridimensional return maps T_{n+2} vs T_{n+1} vs T_n (ms). (a) shows the attractor $E24$ obtained just after the first interior crisis. The red lines are traced orbits starting in region A. The saddle point is in region B, the unstable manifold corresponds to the $B \rightarrow C$ and $B \rightarrow D$ directions. The green spiraling lines are a diagram of a plane stable manifold for the saddle point. (b) shows the attractor $E23$ obtained just before the first interior crisis. The red lines are traced orbits starting in region E. (c) shows the attractor $E34$ obtained just after the second interior crisis. The dense region F of the attractor has crossed the stable manifold of the saddle point.

$E24$ time series. By following point by point the construction of this map we obtained evidence of the existence of a spiraling saddle point close to the region B.

To find the position of the saddle point we traced the orbits from some small regions. We observed that the orbits (red lines) from the small region A evolve to region B and they can only follow the $B \rightarrow C$ or the $B \rightarrow D$ directions, while the orbits from the region just above A are repelled to the $B \rightarrow C$ direction and those just below are repelled to the $B \rightarrow D$ direction. Therefore, we concluded that the saddle point is inside the small region B, and the $B \rightarrow C$ and the $B \rightarrow D$ directions correspond to the unstable manifold, while the stable manifold corresponds to the spiraling orbits that evolve to region B. The green lines are a pictorial representation of the stable manifold.

The saddle point exists for all attractors, but from $E0$ up to $E23$ one can see just the upward deflection due to the saddle repulsion as shown in Fig. 3(b) for $E23$. The sudden change in the $E23 \rightarrow E24$ [Fig. 3(b)$\rightarrow$Fig. 3(a)] transition is due to the transverse crossing of the region A of the attractor through the stable manifold of the saddle. Therefore, the $B \rightarrow D$ direction comes out, defining an interior crisis [13,14] that occurs when the attractor collides with the saddle.

A second interior crisis is observed in the transition $E33 \rightarrow E34$, as shown in Figs. 1(c), 1(d), and 2. In this transition a denser region (F) of the original attractor crosses the stable plane of the saddle as shown in Fig. 3(c).

In conclusion, the existence of a spiraling saddle point and its manifolds was experimentally shown. Two interior crises due to the collisions between the attractors and the stable manifold of the saddle point was also observed.

We are grateful to A. L. Bonini for his suggestions. Financial support from the Brazilian Agencies FAPESP, CAPES, CNPq, and FINEP is gratefully acknowledged.

[1] R. Shaw, *The Dripping Faucet as a Model Chaotic System* (Aerial Press, Santa Cruz, 1984).

[2] P. Martien, S. C. Pope, P. L. Scott, and R. S. Shaw, Phys. Lett. **110A**, 339 (1985).

[3] H. N. N. Yépez, A. L. S. Brito, C. A. Vargas, and L. A. Vicente, Eur. J. Phys. **10**, 99 (1989).

[4] R. F. Cahalan, H. Leidecher, and G. D. Cahalan, Comput. Phys. **4**, 368 (1990).

[5] X. Wu and Z. A. Schelly, Physica D **40**, 433 (1989).

[6] K. Dreyer and F. R. Hickey, Am. J. Physiol. **59**, 619 (1991).

[7] J. C. Sartorelli, W. M. Gonçalves, and R. D. Pinto, Phys. Rev. E **49**, 3963 (1994).

[8] R. D. Pinto, W. M. Gonçalves, J. C. Sartorelli, and M. J. de Oliveira, Phys. Rev. E **52**, 6892 (1995).

[9] T. J. P. Penna, P. M. C. de Oliveira, J. C. Sartorelli, W. M. Gonçalves, and R. D. Pinto, Phys. Rev. E **52**, R2168 (1995).

[10] M. S. F. da Rocha, J. C. Sartorelli, W. M. Gonçalves, and R. D. Pinto, Phys. Rev. E **54**, 2378 (1996).

[11] J. G. M. da Silva, J. C. Sartorelli, W. M. Gonçalves, and R. D. Pinto, Phys. Lett. A **226**, 269 (1996).

[12] H. D. I. Abarbanel, R. Brown, and L. S. Tsimring, Rev. Mod. Phys. **65**, 1331 (1993).

[13] C. Grebogi, E. Ott, and J. A. Yorke, Phys. Rev. Lett. **48**, 1507 (1982); Physica D **7**, 181 (1983).

[14] K. T. Alligood, T. D. Sauer, and J. A. Yorke, *Chaos - An Introduction to Dynamical Systems* (Springer-Verlag, New York, 1997).